Proc. of JSCE,
No. 185, Jan. 1971

SOME STUDIES ON THE MECHANICS OF BED LOAD TRANSPORT

*By Syunsuke IKEDA**

SYNOPSIS

Theoretical expressions of the rolling velocity of a spherical sand grain and of the critical saltation force are derived for steady and uniform flow. In this process, the effect of turbulence and the existence of the viscous sublayer are fully considered. The expressions show fairly good agreement with the experimental results. The effect of turbulence is negligible in the rolling motion. However, it becomes important in the saltation motion. Moreover, more precise expression of the saltation motion of a spherical sand grain is derived by referring to Kishi's method.

1. INTRODUCTION

Many researchers have studied the rate of sediment transport since du Boys to determine the empirical formula by finding the relation between the intensity of bed load transport and the flow intensity.

The ϕ-ψ relation obtained by H.A. Einstein[1] is one of the most popular formula of all the existing methods of determining the rate of bed load transport. This ϕ-ψ relation is derived by assuming that : (1) grain motion is caused by velocity fluctuations, and (2) the average distance traveled by the grains has a constant value and is independent of the flow condition and of the bed composition. The idea that the grains begin to move because of velocity fluctuations is contrary to the experimental evidence that the bed material can begin to move even if the grains are completely contained in the viscous sublayer. The author believes that the average traveling distance is not constant but certain function of the flow and bed composition.

Sato-Kikkawa-Ashida[4] carried out many extensive experiments of bed load transport in a large open channel, 114 m long and 0.78 m wide, and found a relation between bed load function and the coefficient of roughness by considering the physical mechanism of the bed load transport. Their semi-theoretical formula for the rate of bed load transport are very useful in applying to the natural rivers.

Yalin[5] and Kishi-Fukuoka[6] calculated the mean motion of a sand grain analytically on the assumption that the sediment transport in water is dominated by the so-called saltation. On the other hand, Kalinske[7] insisted that the sediment transport by the saltation process is insignificant, therefore need not be considered.

The author believes that the motion of sediment varies from rolling or creep to mainly saltation as the flow intensity increases. Hence the author investigated the mechanics of the mean motion of the grains, that is, the velocity of a spherical sand grain which is rolling on the bed, the critical saltation force and the saltation motion of a spherical sand grain, by considering the forces which are acting on a grain, such as the drag, the lift, the gravity and the friction resulting from the bed.

In this process, the effects of the fluid velocity fluctuations are taken into account by utilizing the theory of turbulence and some experimental results. However, it is considered only for the simplest case, the steady and uniform flow over a fixed bed on which a movable spherical sand grain exists. Hence, in applying to the actual river bed, the effects of the sheltering and the variation of the velocity distribution due to the motion of other sand grains must be considered. The mechanics of these effects are so complicated that they are not estimated dynamically in this paper.

2. FORCES ACTING ON A MOVING SPHERICAL SAND GRAIN

For the sake of simplicity, it is assumed here that the flow on the bed is two-dimensional and the shape of a sand grain is sperical as shown in Fig. 1. Among the forces which act on a spherical sand grain, the drag D, the lift L, the friction from the bed F and the gravity force W are dominant and the other forces are negligible. In order to estimate these

* Graduate Student, Dept. of Civil Engineering, Univ. of Tokyo

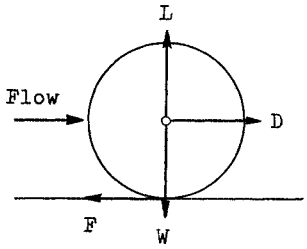

Fig. 1 Schematic diagram of a spherical sand grain.

forces it is necessary to determine the velocity distributions on the bed. According to Rotta[8], in the transition region the total shear stress is determined by viscous and turbulence effects. For the turbulence part he applied Prandtl's mixing length theory, and put

$$\tau=\rho\left(\nu+l^2\left|\frac{\partial \bar{u}}{\partial z}\right|\right)\frac{\partial \bar{u}}{\partial z} \quad \cdots\cdots(1)$$

where τ=shearing stress, ρ=density of fluid, ν=kinematic viscosity, $\bar{u}$=velocity of mean flow, z=distance from the bed, $l=k(z-\delta)$, k=universal constant, and δ=thickness of the viscous sublayer. After integrating Eq. (1) with respect to z, $\bar{u}$ for z reads

$$\frac{\bar{u}}{u_*}=\frac{1}{k\eta}\left(\frac{1}{2}-\sqrt{\eta^2+\frac{1}{4}}\right)+\frac{1}{k}\log_e\left(2\eta+2\sqrt{\eta^2+\frac{1}{4}}\right)+\frac{u_*\delta}{\nu} \quad \cdots\cdots(2)$$

where u_*=friction velocity and $\eta=\frac{l u_*}{\nu}$. In the viscous sublayer, where the flow is completely viscous, the velocity distribution is linear with distance from the bed

$$\frac{\bar{u}}{u_*}=\frac{u_*}{\nu}z \quad \cdots\cdots(3)$$

In the case of fully developed turbulence, the viscous sublayer disappears. The mixing length at $z=0$, however, has some finite value l_0, because of the roughness. Rotta assumed $l=l_0+kz$ to solve Eq. (1). The solution of Eq. (1), under the boundary condition $\bar{u}=0$ at $z=0$, is

$$\frac{\bar{u}}{u_*}=\frac{1}{k\eta}\left(\frac{1}{2}-\sqrt{\eta^2+\frac{1}{4}}\right)-\frac{1}{k\eta_0}\left(\frac{1}{2}-\sqrt{\eta_0^2+\frac{1}{4}}\right)+\frac{1}{k}\log_e\left[\left(\eta+\sqrt{\eta^2+\frac{1}{4}}\right)\Big/\left(\eta_0+\sqrt{\eta_0^2+\frac{1}{4}}\right)\right] \quad \cdots\cdots(4)$$

where $\eta_0=\frac{l_0 u_*}{\nu}$. Nikuradse[9] investigated the velocity distributions of flow through circular pipes with walls of uniform sand grain roughness and got

$$\frac{\bar{u}}{u_*}=A_r+\frac{1}{k}\log_e\frac{u_* z}{\nu}-\frac{1}{k}\log_e\frac{u_* d}{\nu} \quad \cdots\cdots(5)$$

Comparison of expanded form of Eq. (2) with

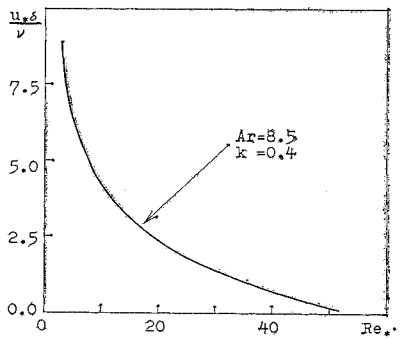

Fig. 2 Relation between $u_*\delta/\nu$ and Re_*.

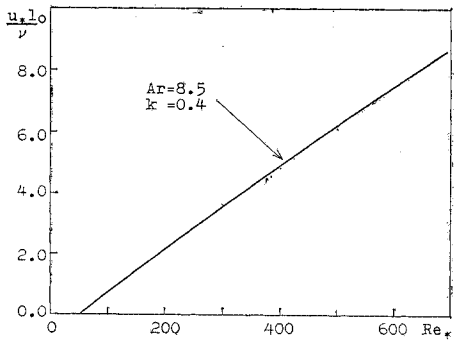

Fig. 3 Relation between $u_* l_0/\nu$ and Re_*.

Eq. (5) for large value of z yields the relation between $\frac{u_*\delta}{\nu}$ and $\frac{u_* d}{\nu}$ as shown in Fig. 2. In the same way, the relation between $\frac{u_* l_0}{\nu}$ and $\frac{u_* d}{\nu}$ can be obtained by comparing Eq. (4) with Eq. (5). This relation is shown in Fig. 3.

Referring to Fig. 2, the shear Reynolds number Re_* can be classified into three parts according to the ratio of the thickness of the viscous sublayer to the diameter of a grain, namely

$$\left.\begin{array}{ll} Re_* \leq 5.5 & ;\ \delta/d \geq 1 \\ 5.5 < Re_* < 51.0 & ;\ 0<\delta/d<1 \\ Re_* \geq 51.0 & ;\ \delta/d=0 \end{array}\right\} \quad \cdots\cdots(6)$$

The drag D, the lift L and the friction force F which are acting on a spherical sand grain can be expressed as follows :

$$\left.\begin{aligned} L&=\frac{\rho}{8}C_L(\bar{u}_1-u_s)^2\pi d^2-\frac{\partial p}{\partial z}(d-\delta)\frac{\pi}{4}\gamma^2 \\ D&=\frac{\rho}{8}C_D(\bar{u}_1-u_s)^2\pi d^2-\frac{\partial p}{\partial x}\gamma\beta\frac{\pi}{4}d^2 \\ F&=\mu\left[(\rho_s-\rho)\frac{\pi}{6}g d^3-L\right] \end{aligned}\right\} \quad \cdots\cdots(7)$$

where C_D=drag coefficient, C_L=lift coefficient, $\bar{u}_1$=fluid velocity at the center of a spherical sand grain, u_s=velocity of a moving spherical sand grain, μ=coefficient of the kinetic friction, x=Cartesian co-ordinate taken in the flow direction, $\frac{\partial p}{\partial x}$, $\frac{\partial p}{\partial z}$

=pressure gradients due to velocity fluctuations, γ =diameter of the cross-section of a spherical sand grain at the edge of the viscous sublayer, and β= ratio of the front area exposed on turbulence to the entire front area of the spherical sand grain exposed to the flow direction. The diagram of γ and β is shown in Fig. 4. Figure 5 shows the values of γ/d and β.

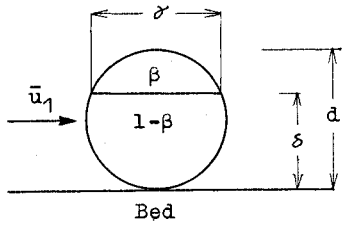

Fig. 4 The diagram of γ and β.

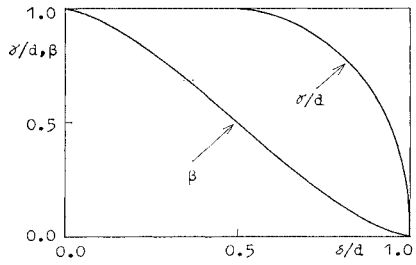

Fig. 5 Relation between δ/d and γ/d, β.

It is assumed that the drag coefficient can be set approximately equal to that of a sphere laid in a uniform flow by neglecting the effect due to the existence of fluid velocity gradient. Concerning the lift coefficient C_L, Chepil[10] conducted fairly detailed experiments on flow through a two-dimensional wind tunnel. The results are shown in Fig. 7. In which, the reader may approve a constant relation between C_L and C_D, namely

$$C_L=0.85\,C_D \quad \cdots\cdots(8)$$

μ was obtained by experiments. The process is as follows :

(1) drop a sphere on a plate to which sand grains or glass beads are tightly attached.

(2) search an angle of slope Θ at which the

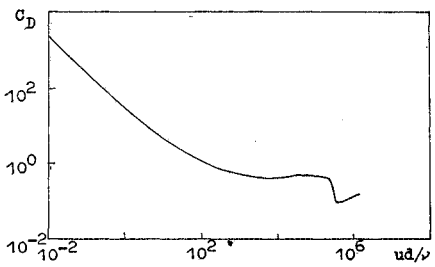

Fig. 6 Relation between C_D of sphere and ud/ν.

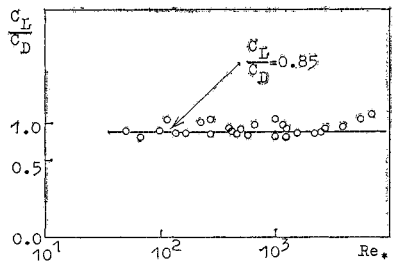

Fig. 7 Relation between C_L/C_D and Re_*.

motion of the sphere obeys mainly rolling. Moreover, at the same time the frequency of jumping motion is nearly equal to that of stop, because the above three types often take place at the same angle.

(3) then, μ can be calculated by using the following relation :

$$\mu=\tan\Theta$$

(4) conduct the same experiment for other sphere with different diameter.

The experiments are performed for two kinds of sands, $K=0.355$ cm and $K=0.402$ cm, and for two kinds of glass beads, $=0.176$ cm and $=0.530$ cm. These experimental results prove that the values of are determined by the ratio d/K and that there is a slight difference between sand and glass bead.

We now proceed to estimate the pressure gradient due to turbulence $\frac{\partial p}{\partial x}$ and $\frac{\partial p}{\partial z}$ as Iwagaki[3] did. In turbulent flows, the viscous effects are negligible, hence Euler's equations of motion must hold at any instant. Then, they read

$$\left.\begin{aligned}-\frac{\partial p}{\partial x}&=\rho\frac{Du}{Dt}\\ -\frac{\partial p}{\partial z}&=\rho\frac{Dw}{Dt}\end{aligned}\right\}\quad\cdots\cdots(9)$$

If it is assumed that the flow is steady and if we adopt the time means of them, then Eq. (9) can be rewritten as follows :

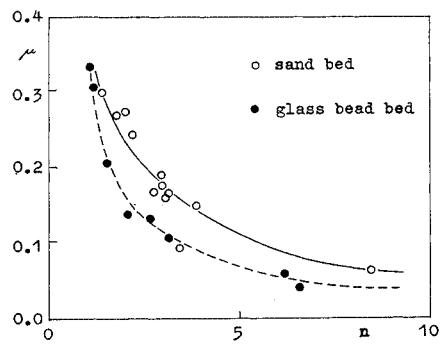

Fig. 8 Relation between coefficient of the kinetic friction and d/K.

$$\left.\begin{aligned} -\frac{1}{\rho}\frac{\partial p}{\partial x} &= \overline{u'\frac{\partial u'}{\partial x}} + \overline{w'\frac{\partial u'}{\partial z}} \\ -\frac{1}{\rho}\frac{\partial p}{\partial z} &= \overline{u'\frac{\partial w'}{\partial x}} + \overline{w'\frac{\partial w'}{\partial z}} \end{aligned}\right\} \cdots\cdots (10)$$

where u', w'=velocity fluctuations of u and w, respectively. As there is no data which gives the correlation coefficients for $u'\frac{\partial u'}{\partial x}$, $w'\frac{\partial u'}{\partial z}$, $u'\frac{\partial w'}{\partial x}$ and $w'\frac{\partial w'}{\partial z}$, it may be allowed to adopt the root mean squares of them. Eq. (10) then reads

$$\left.\begin{aligned} -\frac{1}{\rho}\frac{\partial p}{\partial x} &= \sqrt{\overline{u'^2}}\sqrt{\overline{\left(\frac{\partial u'}{\partial x}\right)^2}} + \sqrt{\overline{w'^2}}\sqrt{\overline{\left(\frac{\partial u'}{\partial z}\right)^2}} \\ -\frac{1}{\rho}\frac{\partial p}{\partial z} &= \sqrt{\overline{u'^2}}\sqrt{\overline{\left(\frac{\partial w'}{\partial x}\right)^2}} + \sqrt{\overline{w'^2}}\sqrt{\overline{\left(\frac{\partial w'}{\partial z}\right)^2}} \end{aligned}\right\} \cdots\cdots (11)$$

For isotropic turbulence, the correlation functions can be developed into Taylor series as follows[11] :

$$\left.\begin{aligned} f_{xx} &= 1-\frac{x^2}{2!\overline{u'^2}}\overline{\left(\frac{\partial u'}{\partial x}\right)^2}+\frac{x^4}{4!\overline{u'^2}}\overline{\left(\frac{\partial^2 u'}{\partial x^2}\right)^2}-\cdots \\ f_{zz} &= 1-\frac{z^2}{2!\overline{w'^2}}\overline{\left(\frac{\partial w'}{\partial z}\right)^2}+\frac{z^4}{4!\overline{w'^2}}\overline{\left(\frac{\partial^2 w'}{\partial z^2}\right)^2}-\cdots \\ g_{xx} &= 1-\frac{x^2}{2!\overline{w'^2}}\overline{\left(\frac{\partial w'}{\partial x}\right)^2}+\frac{x^4}{4!\overline{w'^2}}\overline{\left(\frac{\partial^2 w'}{\partial x^2}\right)^2}-\cdots \\ g_{zz} &= 1-\frac{z^2}{2!\overline{u'^2}}\overline{\left(\frac{\partial u'}{\partial z}\right)^2}+\frac{z^4}{4!\overline{u'^2}}\overline{\left(\frac{\partial^2 u'}{\partial z^2}\right)^2}-\cdots \end{aligned}\right\} \cdots\cdots (12)$$

where f_{xx}, f_{zz}=coefficients of the longitudinal velocity correlations for x and z directions, respectively, and g_{xx}, g_{zz}=coefficients of the lateral velocity correlations for x and z directions, respectively. For very small values of x and z, the correlation functions approach the parabolic functions of x and z. We then obtain

$$\left.\begin{aligned} \frac{1}{2\overline{u'^2}}\overline{\left(\frac{\partial u'}{\partial x}\right)^2} &= \lim_{x\to 0}\frac{1-f_{xx}}{x^2} \\ \frac{1}{2\overline{w'^2}}\overline{\left(\frac{\partial w'}{\partial z}\right)^2} &= \lim_{z\to 0}\frac{1-f_{zz}}{z^2} \\ \frac{1}{2\overline{w'^2}}\overline{\left(\frac{\partial w'}{\partial x}\right)^2} &= \lim_{x\to 0}\frac{1-g_{xx}}{x^2} \\ \frac{1}{2\overline{u'^2}}\overline{\left(\frac{\partial u'}{\partial z}\right)^2} &= \lim_{z\to 0}\frac{1-g_{zz}}{z^2} \end{aligned}\right\} \cdots\cdots (13)$$

The terms on the right hand side are called micro scale of eddies as well known in the theory of turbulence. Introducing λ_f and λ_g as the micro scales of eddies and considering $\lambda_f=\sqrt{2}\,\lambda_g$ for isotropic turbulence, we have for small values of x and z

$$\left.\begin{aligned} \overline{\left(\frac{\partial u'}{\partial x}\right)^2} &= \frac{\overline{u'^2}}{\lambda_g^2} \\ \overline{\left(\frac{\partial w'}{\partial z}\right)^2} &= \frac{\overline{w'^2}}{\lambda_g^2} \\ \overline{\left(\frac{\partial w'}{\partial x}\right)^2} &= 2\frac{\overline{w'^2}}{\lambda_g^2} \\ \overline{\left(\frac{\partial u'}{\partial z}\right)^2} &= 2\frac{\overline{u'^2}}{\lambda_g^2} \end{aligned}\right\} \cdots\cdots (14)$$

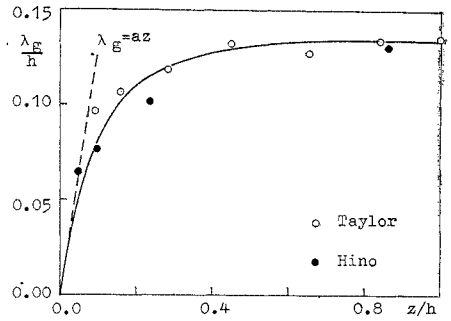

Fig. 9 Distribution of the micro scale of eddies.

Taylor[12] made measurement on spatial correlations for flow in a two-dimensional channel. The experimental results are shown in Fig. 9. It may be noticed that the micro scale of eddies λ_g shows a linear increase with distance z near the wall. Then λ_g can be written in the region close to the wall as follows :

$$\lambda_g = az+\lambda_0 \cdots\cdots (15)$$

where λ_0=increase of λ_g due to the roughness of the bed.

Klebanoff[13] and Corrsin & Kistler[14] measured the intensities of the velocity fluctuations in wind tunnels. Their experimental results are shown Fig. 10. In this figure, considering $u'=2w'$ near the wall, it can be obtained

$$\left.\begin{aligned} \frac{u'}{u_*} &= 2.1-0.00054\frac{u_* z}{\nu} \\ \frac{w'}{u_*} &= 1.05-0.00027\frac{u_* z}{\nu} \end{aligned}\right\} \cdots\cdots (16)$$

Substituting Eqs. (14), (15) and (16) into Eq. (11), we have

$$\left.\begin{aligned} -\left(\frac{\partial p}{\partial x}\right)_{(a+\delta)/2} &= \frac{1.707\,\rho\,u_*^2}{az+\lambda_0}\times\left[2.1-0.00027\frac{u_*(d+\delta)}{\nu}\right]^2 \\ -\left(\frac{\partial p}{\partial z}\right)_{(a+\delta)/2} &= \frac{0.957\,\rho\,u_*^2}{az+\lambda_0}\times\left[2.1-0.00027\frac{u_*(d+\delta)}{\nu}\right]^2 \end{aligned}\right\} \cdots\cdots (17)$$

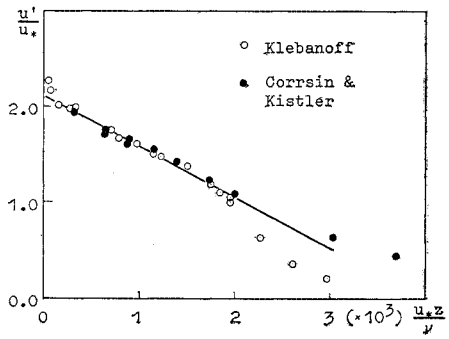

Fig. 10 Distribution of u'.

Then L, D and F read

$$\left.\begin{aligned} L&=\frac{\rho}{8}C_L(\bar{u}_1-u_s)^2\pi d^2+\frac{0.957\,\rho u_*^2}{\frac{a}{2}(d+\delta)+\lambda_0}\\ &\times\left[2.1-0.00027\frac{u_*(d+\delta)}{\nu}\right]^2(d-\delta)\frac{\pi}{4}r^2\\ D&=\frac{\rho}{8}C_D(\bar{u}_1-u_s)^2\pi d^2+\frac{1.707\,\rho u_*^2}{\frac{a}{2}(d+\delta)+\lambda_0}\\ &\times\left[2.1-0.00027\frac{u_*(d+\delta)}{\nu}\right]^2 r\beta\frac{\pi}{4}d^2\\ F&=\mu\left[(\rho_s-\rho)\frac{\pi}{\sigma}g\,d^3-L\right] \end{aligned}\right\} \quad \cdots\cdots(18)$$

These are the expressions of the forces which are acting on a spherical sand grain rolling on the bed.

3. THE VELOCITY OF A ROLLING SPHERICAL SAND GRAIN

The sand grains on the bed begin to roll when the tractive force surpasses the critical tractive force. The fundamental equation of motion for a rolling grain can be expressed as follows, since the effect due to rolling is adjusted in μ experimentally

$$M\frac{du_s}{dt}=-F+D-\frac{1}{2}m\frac{du_s}{dt} \quad \cdots\cdots(19)$$

where M=mass of a spherical sand grain $\left(=\frac{\pi}{6}\rho_s d^3\right)$, and m=virtual mass due to acceleration $\left(=\frac{\pi}{6}\rho d^3\right)$. Substitution of Eq. (18) into Eq. (19) gives

$$\left.\begin{aligned} \frac{du_s}{dt}&=\frac{3}{4}(\mu C_L+C_D)(\bar{u}_1-u_s)^2\Big/\left(\rho_s/\rho+\frac{1}{2}\right)d\\ &-\left\{\mu(\rho_s/\rho-1)g-\frac{3}{2}\left[0.957\,\mu\left(1-\frac{\delta}{d}\right)\left(\frac{r}{d}\right)^2\right.\right.\\ &\left.\left.+1.707\frac{r}{d}\beta\right]\cdot\left[2.1-0.00027\frac{u_*(d+\delta)}{\nu}\right]^2\right.\\ &\left.\times\frac{u_*^2}{\frac{a}{2}(d+\delta)+\lambda_0}\right\}\Big/\left(\rho_s/\rho+\frac{1}{2}\right) \end{aligned}\right\} \quad \cdots\cdots(20)$$

The solution of Eq. (20), under the intial condition $u_s=0$ at $t=0$, is

$$t=\frac{1}{2\sqrt{fh}}\log_e\left|\frac{[h(u_s-\bar{u}_1)-\sqrt{fh}][h\bar{u}_1-\sqrt{fh}]}{[h(u_s-\bar{u}_1)+\sqrt{fh}][h\bar{u}_1+\sqrt{fh}]}\right| \quad \cdots\cdots(21)$$

where

$$\begin{aligned} f&=\left\{\mu(\rho_s/\rho-1)g-\frac{3}{2}\left[0.957\,\mu\left(1-\frac{\delta}{d}\right)\left(\frac{r}{d}\right)^2\right.\right.\\ &\left.\left.+1.707\frac{r}{d}\beta\right]\cdot\left[2.1-0.00027\frac{u_*(d+\delta)}{\nu}\right]^2\right.\\ &\left.\times\frac{u_*^2}{\frac{a}{2}(d+\delta)+\lambda_0}\right\}\Big/\left(\rho_s/\rho+\frac{1}{2}\right)\\ h&=\frac{3}{4}(\mu C_L+C_D)\Big/\left(\rho_s/\rho+\frac{1}{2}\right)d \end{aligned}$$

For very large value of t, that is, the steady condition, Eq. (21) yields

$$\frac{u_s}{u_*}=\frac{\bar{u}_1}{u_*}-\frac{1}{u_*}\sqrt{\frac{f}{h}} \quad \cdots\cdots(22)$$

The reader may notice that this relation coincides with the relation which Kalinske[7] assumed.

It is shown in the following considerations that each term contained in Eq. (22) is the function of u_*d/ν except for $\mu(\rho_s/\rho-1)gd/u_*^2$.

(1) $\bar{u}_1/u_*$ can be calculated by utilizing Eqs. (2), (3) and (4) in accordance with the value of Re_*. In these equations, $u_*\delta/\nu$ and u_*l_0/ν can be determined by referring to Fig. 2 and Fig. 3, respectively. Thus, $\bar{u}_1/u_*$ is the function of Re_*.

(2) δ/d is the function of Re_*, since it can be rewritten as $\frac{u_*\delta}{\nu}\Big/\frac{u_*d}{\nu}$.

(3) r/d and β are determined by the value of δ/d. Hence, they are finally the function of Re_*.

(4) If it is assumed that $\lambda_0=l_0$, $\lambda_0 d/\nu$ reduces to the function of Re_*.

(5) Figure 6 gives the relation between C_D and $\bar{u}_1 d/\nu$. As $\bar{u}_1 d/\nu$ is equal to $\frac{\bar{u}_1}{u_*}\frac{u_*d}{\nu}$, C_D is determined by Re_*.

(6) As defined in Eq. (8), C_L has a constant relation with C_D. Hence, C_L is determined by Re_*.

(7) The term $\mu(\rho_s/\rho-1)gd/u_*^2$ is determined by both the characteristics of the grains which compose the bed and the friction velocity u_*.

(8) μ is obtained by experiments and the original data are used in calculation.

Thus, it is concluded that u_s/u_* is the functions of both Re_* and $\mu(\rho_s/\rho-1)gd/u_*^2$.

The calculation of u_s/u_* is performed by utilizing the gradual approximation method, since the drag coefficient C_D is the function of relative velocity $(\bar{u}_1-u_s)$. The results thus obtained are compared with experimental data in Figs. 12 and 13.

4. THE CRITICAL SALTATION FORCE

As the tractive force increases, the motion of sand grains follows the saltation rather than the rolling. However, it is very difficult to distinguish clearly the difference between the saltation motion and the rolling motion, since they often coexist. In this paper, it is assumed that the saltation motion begins when the lift force overcomes the weight of a spherical sand grain. The boundary of them is investigated in accordance with the ratio δ/d.

(a) $Re_*\leq 5.5$ $(\delta/d\geq 1)$

In this case a spherical sand grain is contained completely in the viscous sublayer and consequently there is no effect due to turbulence. The equilibrium condition $L=W$ gives

$$\frac{\rho}{8}C_L\bar{u}_1^2\pi d^2=\frac{\pi}{6}(\rho_s-\rho)gd^3 \quad \cdots\cdots(23)$$

The velocity $\bar{u}_1$ at the center of a spherical sand

grain can be calculated by utilizing Eq. (3), then we obtain after some calculation

$$\frac{u_*^2}{(\rho_s/\rho-1)g\,d}=\frac{1}{\varphi} \quad \cdots\cdots (24)$$

$$\varphi=\frac{3}{16}C_L\left(\frac{u_*d}{\nu}\right)^2 \quad \cdots\cdots (25)$$

(b) $5.5<Re_*\leq 8.8 (0<\delta/d\leq 1/2)$

The center of a spherical sand grain is still contained in the viscous sublayer, therefore Eq. (3) must be used in calculating the fluid velocity $\bar{u}_1$ in this case, too. However, we must take account of the turbulence effect for the part protruding beyond the viscous sublayer. Thus φ can be obtained in the same way as the case of (a)

$$\varphi=\frac{3}{16}C_L\left(\frac{u_*d}{\nu}\right)^2+\frac{1.436(1-\delta/d)}{\frac{a}{2}\left(1+\frac{\delta}{d}\right)+\frac{\lambda_0}{d}}\times\left[2.1-0.00027\frac{u_*(d+\delta)}{\nu}\right]^2\left(\frac{r}{d}\right)^2 \quad \cdots\cdots (26)$$

(c) $8.8<Re_*<51.0$ $(1/2<\delta/d<1)$

In this case the center of a spherical sand grain is outside the viscous sublayer. Hence, Eq. (2) must be used for calculation of $\bar{u}_1$. We then have the following expression for φ :

$$\left.\begin{aligned}\varphi=\frac{3}{4}C_L\Bigg\{&\frac{1}{k\eta}\left[\frac{1}{2}-\sqrt{\eta^2+\frac{1}{4}}\right]\\&+\frac{1}{k}\log_e\left[2\eta+2\sqrt{\eta^2+\frac{1}{4}}\right]+\frac{u_*\delta}{\nu}\Bigg\}^2\\&+\frac{1.436(1-\delta/d)}{\frac{a}{2}\left(1+\frac{\delta}{d}\right)+\frac{\lambda_0}{d}}(2.1-0.00027\,Re_*)^2\end{aligned}\right\} \quad \cdots\cdots (27)$$

(d) $Re_*\geq 51.0$ $(\delta/d=0)$

As the flow is completely turbulent, Eq.(4) must be used in calculating $\bar{u}_1$. Then φ becomes

$$\left.\begin{aligned}\varphi=\frac{3}{4}C_L\Bigg\{&\frac{1}{k\eta}\left(\frac{1}{2}-\sqrt{\eta^2+\frac{1}{4}}\right)\\&-\frac{1}{k\eta_0}\left(\frac{1}{2}-\sqrt{\eta^2+\frac{1}{4}}\right)+\frac{1}{k}\log_e\\&\left[\left(\eta+\sqrt{\eta^2+\frac{1}{4}}\right)\Big/\left(\eta_0+\sqrt{\eta_0^2+\frac{1}{4}}\right)\right]\Bigg\}^2\\&+\frac{1.436}{\frac{a}{2}+\frac{\lambda_0}{d}}(2.1-0.00027\,Re_*)^2\end{aligned}\right\} \quad \cdots\cdots (28)$$

Thus, the expressions of the critical saltation force are obtained for all the range of Re_*. Figure 14 shows the theoretical curves for $u_*^2/(\rho_s/\rho-1)gd$ as a function of Re_* and the experimental results obtained in a two-dimensional channel.

5. THE SALTATION MOTION OF A SPHERICAL SAND GRAIN

Saltation motion is the most popular type of the bed load transport. Many investigators, such as Bagnold[15], Yalin and Kishi investigated this phenomenon analytically. Here a spherical sand grain which is jumping along the bed by the lift and drag force are investigated. Moreover, it is assumed that the effects of the velocity fluctuations due to turbulence are negligible during the jump. Then, the fundamental equations of motion which hold for the saltation motion of a spherical sand grain are

$$M\frac{du_{sx}}{dt}=D_x-\frac{1}{2}m\frac{du_{sx}}{dt} \quad (x\text{-direction}) \quad (29)$$

$$\left.\begin{aligned}M\frac{du_{sz}}{dt}&=L-W-D_z-\frac{1}{2}m\frac{du_{sz}}{dt}\\&\quad\left(\begin{matrix}z\text{-direction during}\\\text{the upward motion}\end{matrix}\right)\end{aligned}\right\} \quad \cdots\cdots (30\text{-a})$$

$$\left.\begin{aligned}&=L-W+D_z-\frac{1}{2}m\frac{du_{sz}}{dt}\\&\quad\left(\begin{matrix}z\text{-direction during}\\\text{the downward motion}\end{matrix}\right)\end{aligned}\right\} \quad \cdots\cdots (30\text{-b})$$

where M=mass of a spherical sand grain, m=virtual mass, and u_{sx}, u_{sz}=velocity of a grain in the x- and z-directions, respectively.

We now introduce the following new variables to get the dimensionless differential equations :

$$\xi=\frac{x}{d},\quad \zeta=\frac{z}{d},\quad \varepsilon=\frac{\rho}{\rho_s},\quad \sigma=\frac{3}{2}\frac{C_D}{\alpha}\varepsilon,$$

$$D_x=\frac{\rho\,C_{Dx}}{8}(\bar{u}_1-u_s)^2\pi\,d^2,$$

$$D_z=\frac{\rho\,C_{Dz}}{8}(\bar{u}_1-u_s)\pi\,d^2,\quad M=\frac{\pi}{6}\rho_s d^3$$

$$m=\frac{\pi}{6}\rho\,d^3,\quad \theta=\frac{3}{4}\frac{C_D\varepsilon}{d}u_*t,\quad \frac{L}{W}=Yc^{-\alpha\zeta}$$

Substitution of these variables in Eqs. (29), (30-a) and (30-b) yields

$$\frac{d}{d\theta}\frac{u_{sx}}{u_*}=\frac{2}{2+\varepsilon}\left(\frac{\bar{u}_1}{u_*}\right)^2\left(1-\frac{u_{sx}}{\bar{u}_1}\right)^2 \quad \cdots\cdots (31)$$

$$\frac{d}{d\zeta}\left(\frac{u_{sz}}{u_*}\right)^2+\frac{2\alpha\sigma}{2+\varepsilon}\left(\frac{u_{sz}}{u_*}\right)^2=\frac{4\varepsilon\varphi}{2+\varepsilon}(Yc^{-\alpha\zeta}-1) \quad \cdots\cdots (32\text{-a})$$

$$\frac{d}{d\zeta}\left(\frac{u_{sz}}{u_*}\right)^2-\frac{2\alpha\sigma}{2+\varepsilon}\left(\frac{u_{sz}}{u_*}\right)^2=\frac{4\varepsilon\varphi}{2+\varepsilon}(Yc^{-\alpha\zeta}-1) \quad \cdots\cdots (32\text{-b})$$

Now integrate Eq. (31) with respect to u_{sx}/u_* from 0 to u_{sx}/u_*. We then obtain

$$\theta=\left(1+\frac{1}{2}\varepsilon\right)\int_0^{u_{sx}/u_*}\frac{d\left(\frac{u_{sx}}{u_*}\right)}{\left(\frac{\bar{u}_1}{u_*}\right)^2\left(1-\frac{u_{sx}}{u_*}\right)^2} \quad \cdots (33)$$

If it is assumed $\bar{u}_1/u_*=$const., then it follows that

$$\xi=\frac{4}{3\,C_{Dx}\,\varepsilon}\left[\frac{\bar{u}_1}{u_*}\theta+\left(1+\frac{1}{2}\varepsilon\right)\log_e\frac{1+\frac{1}{2}\varepsilon}{1+\frac{1}{2}\varepsilon+\frac{\bar{u}_1}{u_*}\theta}\right] \quad \cdots\cdots (34)$$

which gives the relation between dimensionless time θ and distance ξ.

After solving Eqs. (32-a) and (32-b) under the initial conditions $u_{sz}=0$ at $\zeta=0$ and $u_{sz}=0$ at $\zeta=\zeta_{max}$, respectively, u_{sz} is obtained as follows :

$$\frac{u_{sz}}{u_*}=\left\{\frac{2\varepsilon\varphi}{\alpha}\left[\left(\frac{1}{\sigma}-\frac{2Y}{2\sigma-2-\varepsilon}\right)e^{\frac{-2\alpha\sigma}{2+\varepsilon}\zeta}-\frac{1}{\sigma}+\frac{2Y}{2\sigma-2-\varepsilon}e^{-\alpha\zeta}\right]\right\}^{1/2} \quad \cdots\cdots(35\text{-a})$$

$$\frac{u_{sz}}{u_*}=\left\{\frac{2\varepsilon\varphi}{\alpha}\left[\left(\frac{2Y}{2\sigma+2+\varepsilon}e^{-\alpha\zeta_{max}}-\frac{1}{\sigma}\right)e^{\frac{-2\alpha\sigma}{2+\varepsilon}(\zeta_{max}-\zeta)}+\frac{1}{\sigma}-\frac{2Y}{2\sigma+2+\varepsilon}e^{-\alpha\zeta}\right]\right\}^{1/2} \quad \cdots\cdots(35\text{-b})$$

These solutions are so complicated that the analytical solution of direct relation between θ and ζ can not be obtained. However, it is possible to perform the numerical integration by utilizing the following relation

$$d\zeta=\frac{u_{sz}}{u_*}\frac{4}{3C_{Dz}\varepsilon}d\theta \quad \cdots\cdots(36)$$

Figure 11 represents the moving pattern of a spherical sand grain which is calculated by utilizing a digital computer.

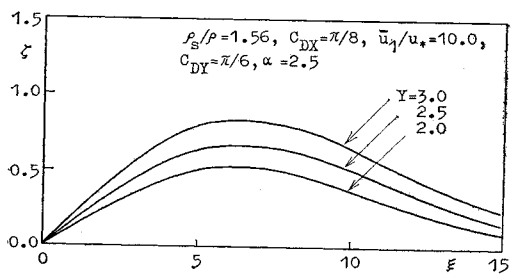

Fig. 11 Saltation motion of a sphericals and grain.

6. COMPARISON WITH EXPERIMENTAL DATA

Experiments are conducted on a two-dimensional open channel, 1 000 cm long and 30 cm wide, to the bottom of which coarse sand grains with mean diameter $K=0.355$ cm are tightly attached. Thus, the bed is fully roughened. Two kinds of spherical sand grains, with diameter 0.5 cm ($\rho_s=1.34$ gr/cm^3) and 0.625 cm ($\rho_s=1.39$ gr/cm^3), are used to measure the transport velocity and to observe the moving pattern of a grain. The transport velocity is measured by a stop watch in a test section, 200 cm long, situated at the middle of the channel.

Fluid velocity distribution, consequently the friction velocity u_*, is measured by utilizing a Pitot-tube of outer diameter 0.2 cm. u_* is calculated from the logarithmic velocity distribution law shown below :

$$\frac{\bar{u}}{u_*}=\frac{1}{k}\log_e\frac{z}{k_s}+B$$

Figures 12 and 13 show the comparison of experimental data of the transport velocity with the

Table 1 Summary of experimental data

Run	d (cm)	u_* (cm/s)	Re_*	u_s/u_*	$\frac{u^2_*}{(\rho_s/\rho-1)gd}$	the pattern of movement
1	0.50	2.17	90	0	0.0277	stop
2	0.50	2.71	113	1.53	0.0434	roll
3	0.50	2.84	118	2.31	0.0476	roll
4	0.50	2.91	121	2.36	0.0500	roll
5	0.50	2.96	119	2.04	0.0458	roll
6	0.50	3.29	132	5.23	0.0566	saltation
7	0.50	4.52	181	3.98	0.107	saltation
8	0.50	5.08	211	4.71	0.152	saltation
9	0.625	1.43	81	0	0.0086	stop
10	0.625	2.17	113	0	0.020	stop
11	0.625	2.54	129	2.70	0.0274	roll
12	0.625	2.71	141	2.61	0.0311	roll
13	0.625	2.77	157	3.45	0.0324	roll
14	0.625	2.84	148	2.61	0.0342	roll
15	0.625	2.91	151	2.79	0.0359	roll
16	0.625	2.96	161	2.86	0.0498	roll
17	0.625	3.48	198	2.66	0.0512	saltation
18	0.625	3.60	205	3.15	0.0548	saltation
19	0.625	4.92	235	6.30	0.103	saltation
20	0.625	5.08	264	5.12	0.109	saltation
21	0.625	7.54	393	7.95	0.241	saltation

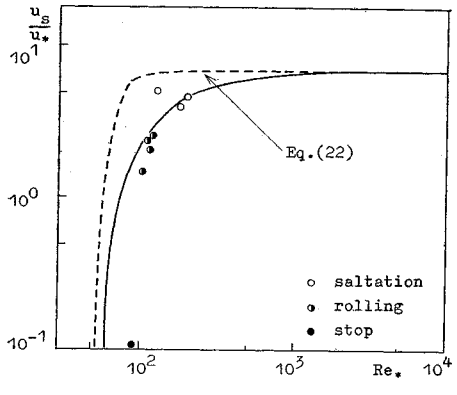

Fig. 12 (d=0.5 cm)

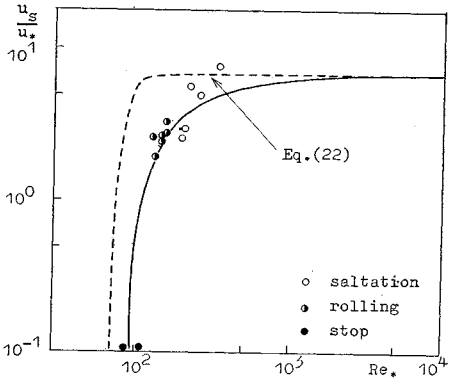

Fig. 13 (d=0.625 cm)

Comparison of experimental results with the theoretical curves for velocity of spherical sand grain.

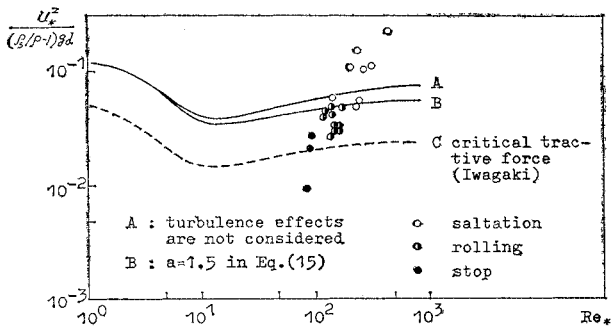

Fig. 14 Comparison of experimental results with theoretical curves for critical saltation force.

theoretical curves obtained from Eq. (22). In which the solid lines are calculated by neglecting the turbulence term in Eq. (22), namely

$$\frac{u_s}{u_*}=\frac{\bar{u}_1}{u_*}-\left[\frac{\mu(\rho_s/\rho-1)}{\frac{3}{4}(\mu C_L+C_D)}\frac{g\,d}{u_*^2}\right]^{1/2}$$

On the other hand, the dotted lines are calculated based on Eq. (22). The reader may notice that the experimental results for rolling motion show better agreement with the solid lines than with the dotted lines. This fact implies that the role of pressure gradient due to turbulence is small and negligible in considering the transport velocity of a grain. It is considered that these turbulence effects are compensated during the long term contact with turbulence, since the turbulence has an isotropic character in the flow direction.

Figure 14 shows a comparison of the critical saltation force obtained from Eqs. (24), (25), (26), (27) and (28) with the experimental results. In this case, on the contrary to the previous, the role of turbulence may be important. The downward component of turbulence is diminished by the existence of the bed and only the upward component is effective for picking up a grain. The curve-B shows good agreement with the experiment. However, the turbulence on the river bed has an nonisotropic character on the contrary to the assumption of isotropy in this paper. Hence, the nonisotropy causes an effect on the saltation of a spherical sand grain, even if it is small. Moreover, in applying to the actual erodible bed such as river the effects of other moving grains must be considered. Iwagaki explained these effects by introducing sheltering coefficient. In this paper the author does not treat the effects of other moving grains, since their mechanics are so complicated that they must be investigated more accurately.

7. CONCLUSIONS

Through the investigations mentioned above, the author finds some interesting and remarkable facts as follows :

(1) The drag coefficient of a sphere laid in a uniform flow is applicable to that of a spherical grain moving on the bed.

(2) The lift coefficient obtained by Chepil is appropriate, because the theoretical expressions of the rolling velocity and the critical saltation force agree with the experiments.

(3) The transport velocity of a spherical grain moving on the bed is not affected by the pressure gradient due to turbulence and is well expressed by

$$\frac{u_s}{u_*}=\frac{\bar{u}_1}{u_*}-\left[\frac{\mu(\rho_s/\rho-1)}{\frac{3}{4}(\mu C_L+C_D)}\frac{g\,d}{u_*^2}\right]^{1/2}$$

This expression coincides with the formula which Kalinske assumed and the second term on the right-hand side corresponds to his critical fluid velocity.

(4) Turbulence is influential in the estimation of the critical saltation force.

8. ACKNOWLEDGEMENT

The many useful instructions and criticisms of Professor Yutaka Takahashi and Lecturer Nobuyuki Tamai, University of Tokyo, are gratefully acknowledged. The author also wishes to express his hearty thanks to Professor Hideo Kikkawa, Tokyo Institute of Technology, for his creative criticisms.

REFERENCES

1) Einstein, H.A. : The Bed-Load Function for Sediment Transportation in Open Channel Flows, U.S. Department of Agriculture, Soil Conservation Service, Tech. Bulletin, No. 1026, 1950.
2) Rouse, H. : Engineering Hydraulics, John Wiley & Sons, Inc., 1965.
3) Iwagaki, Y. : Fundamental Study on Critical Tractive Force, Trans. J.S.C.E., No. 41, 1956. (in Japanese)
4) Sato, S., Kikkawa, H. & Ashida, K. : Study on the Bed-Load Transportation, Report of Research Institute for Civil engineering, No. 98, 1956 (in Japanese)
5) Yalin, M.S. : An Expression for Bed-Load Transportation, Proc. of A.S.C.E., Hy 3, May 1963.
6) Kishi, T. & Fukuoka, S. : Saltation Mechanism of Bed-Load and its Rate, The 10th Japanese Conference on Hydraulies, J.S.C.E., 1966 (in Japanese)
7) Kalinske, A. A. : Movement of Sediment as Bed Load in Rivers, Trans. A. G. U., Vol. 28, No. 4, August 1947.
8) Rotta, J. : Das in Wandnähe gültige Beschwindigkeitsgesetz turbulenter Strömungen, Ingenieur Archiv, 18 Band, 1950.
9) Nikuradse, J. : Strömungsgesetze in rauhen Rohren, Forschungsheft 361, 1933; see also Boundary Layer Theory, Schlichting, McGRAW-HILL, 1962.
10) Chepil, W.S. : The Use of Evenly Spaced Hemispheres to Evaluate Aerodynamic Forces on a Soil Sur-

face, Trans. A.G.U., Vol. 39, No. 3, June 1958.
11) Hinze, J.O. : Turbulence, McGRAW-HILL, 1959.
12) Taylor, G.I. : Statistical Theory of Turbulence, Part 3, Distribution of Dissipation of Energy in Pipe over its Cross-Section, Proc. of Roy. Soc, A, 151, 1935.
13) Klebanoff, P.S. : NACA Tech. Notes 3178, 1954.
14) Corrsin, S. & Kistler, A.S. : NACA Tech. Notes 3178, 1954
15) Bagnold, R.A. : The Movement of Desert Sand, Proc. of Roy. Soc., A, 892, Vol. 157, 1936.

APPENDIX.-NOTATION

a : numerical coefficient
C_D : drag coefficient
C_L : lift coefficient
d : diameter of the sand grain
D : drag
f_{xx}, f_{zz} : coefficients of the longitudinal velocity correlations for x and z directions
F : friction from the bed
g : acceleration due to gravity
g_{xx}, g_{zz} : coefficients of the lateral velocity correlations for x and z directions
k : universal constant
K : roughness of the bed
l : mixing length
l_0 : increase of the mixing length due to the roughness of the bed
L : lift
m : virtual mass due to acceleration
M : mass of a spherical sand grain
Re_* : shear Reynolds number
t : time
$\bar{u}$: velocity of mean flow
$\bar{u}_1$: fluid velocity at the center of a spherical sand grain
u_s : velocity of a moving spherical sand grain
u_* : friction velocity
u', w' : velocity fluctuations
x : Cartesian co-ordinate taken in the flow direction
z : distance from the bed
α : constant considering the intensity of the variation of L/W with the dimensionless distance z/d
β : ratio of the front area exposed on turbulence to the entire front area of the spherical sand grain exposed to the flow direction
γ : diameter of the cross-section of a spherical sand grain at the edge of the viscous sublayer
δ : thickness of the viscous sublayer
ε : ρ/ρ_s
ζ : z/d
η : lu_*/ν
η_0 : $l_0 u_*/\nu$
θ : $3\,C_D\,\varepsilon\,u_* t/4\,d$
λ_f, λ_g : micro scale of eddies
μ : coefficient of the kinetic friction
ν : kinematic viscosity
ξ : x/d
ρ : density of fluid
σ : $3\,C_D\,\varepsilon/2\,\alpha$
τ : shear stress

(Received June 2, 1970)